



AALBORG UNIVERSITY
DENMARK

Aalborg Universitet

The Impact of Riser-induced Slugs on the Downstream Deoiling Efficiency

Pedersen, Simon; Bram, Mads Valentin

Published in:
Journal of Marine Science and Engineering

DOI (link to publication from Publisher):
[10.3390/jmse9040391](https://doi.org/10.3390/jmse9040391)

Creative Commons License
CC BY 4.0

Publication date:
2021

Document Version
Publisher's PDF, also known as Version of record

[Link to publication from Aalborg University](#)

Citation for published version (APA):
Pedersen, S., & Bram, M. V. (2021). The Impact of Riser-induced Slugs on the Downstream Deoiling Efficiency. *Journal of Marine Science and Engineering*, 9(4), [391]. <https://doi.org/10.3390/jmse9040391>

General rights

Copyright and moral rights for the publications made accessible in the public portal are retained by the authors and/or other copyright owners and it is a condition of accessing publications that users recognise and abide by the legal requirements associated with these rights.



- Users may download and print one copy of any publication from the public portal for the purpose of private study or research.
- You may not further distribute the material or use it for any profit-making activity or commercial gain
- You may freely distribute the URL identifying the publication in the public portal -

Take down policy

If you believe that this document breaches copyright please contact us at vbn@aub.aau.dk providing details, and we will remove access to the work immediately and investigate your claim.

Article

The Impact of Riser-Induced Slugs on the Downstream Deoiling Efficiency

Simon Pedersen *  and Mads Valentin Bram 

Department of Energy Technology, Aalborg University, Niels Bohrs Vej 8, 6700 Esbjerg, Denmark; mvb@et.aau.dk
* Correspondence: spe@et.aau.dk; Tel.: +45-9940-3376

Abstract: In Oil and gas productions, the severe slug is an undesired flow regime due to the negative impact on the production rate and facility safety. This study examines the severe riser-induced slugs' influence on a typical separation process, consisting of a 3-phase gravity separator physically linked to a deoiling hydrocyclone. Four inflow scenarios are compared: Uncontrolled, open-loop, feasible, and infeasible closed-loop anti-slug control, respectively. Three PID controllers' coefficients are kept constant for all the tests: The separator pressure, water level, and hydrocyclone pressure-drop-ratio (PDR) controllers. The simulation results show that the separation efficiency is significantly larger in the closed-loop configuration, probably due to the larger production rates which provide a preferable operation condition for the hydrocyclone. It is concluded that both slug elimination approaches improve the separation efficiency consistency, but that the closed-loop control provides the best overall separation performance.

Keywords: oil and gas; multi-phase flow; anti-slug; riser slug; separation; deoiling; hydrocyclone; stabilization



Citation: Pedersen, S.; Bram, M.V. The Impact of Riser-Induced Slugs on the Downstream Deoiling Efficiency. *J. Mar. Sci. Eng.* **2021**, *9*, 391. <https://doi.org/10.3390/jmse9040391>

Academic Editor: Malcolm L. Spaulding

Received: 8 March 2021
Accepted: 31 March 2021
Published: 7 April 2021

Publisher's Note: MDPI stays neutral with regard to jurisdictional claims in published maps and institutional affiliations.



Copyright: © 2020 by the authors. Licensee MDPI, Basel, Switzerland. This article is an open access article distributed under the terms and conditions of the Creative Commons Attribution (CC BY) license (<https://creativecommons.org/licenses/by/4.0/>).

1. Introduction

In offshore Oil and gas installations, severe slug is an undesired flow regime in the well-pipeline-riser systems, as it has proved to have negative impact on the daily production [1–3]. The issues related to the severe slugs are numerous [4]: Overload on gas compressors, fatigue in the transportation pipelines, increased corrosion [5–7], production reduction [8], production stop and high pressure and liquid overflow in the downstream gravity separators [9]. Anti-slug feedback control is one effective solution for changing the slug flow to a stable flow regime [10]. A common approach is to stabilize the fluctuating pressure and/or flow by manipulating the topside choke valve at the riser top [11,12]. However, as the controllers lack robustness to process or condition changes, the operators sometimes manually choke the valves to conservatively low opening degrees to eliminate the severe slugs with the consequence of simultaneously reducing the productions [13].

The traditional separation technology in the North Sea consists of 3-phase gravity separators and deoiling hydrocyclones. This configuration represents 90% of the existing deoiling technologies in the North Sea [14]. The outlet of a well-pipeline-riser transportation process is typically physically linked to a 3-phase gas/water/oil gravity separator. The first step in the separation consists of a single or multiple stage 3-phase separators to completely separate the gas and separate most of the oil in the water. The water outlet of the last 3-phase separator is connected to a deoiling facility consisting of multiple hydrocyclone liners [15,16].

The highly fluctuating production rate induced by severe slugs occurring in the riser can cause liquid overflow in the 3-phase separator if the separator's size is designed for a non-slugging buffer time [9]. Furthermore, the study from [15] proved that a poor separation in the separator will affect the performance in the rest of the typical produced water separation process. Thus, handling the slugs upstream the separator would be preferable as the slugs can reduce the separation efficiency of the separator, ultimately

resulting in a limited production rate, reduced production quality, as well as difficulties and challenges for the produced water treatment. The study in [17] proposed control methods for the gravity separator outlet valves to handle the large slug disturbances to the separation process. However, the work only investigate the gravity separator isolated with no downstream deoiling separation included. To the best of the author's knowledge there are no practical studies on slug's effects on deoiling performance of the hydrocyclone; however, there has been several empirical [18–20] and mathematical [21–25] on hydrocyclone operation and efficiency. Generally they agree that the splitting of the flow in the hydrocyclone is proportional to the pressure drop ratio [26,27].

This paper will examine the relationship between severe slugs (under different running conditions) and the associated produced water treatment performance. A testing facility is used to test both the transportation and the separator-hydrocyclone separation systems [28–30]. The work examined in [31] concluded that the separation performance decreased when severe riser-induced slugs are presents, however, the oil-in-water (OiW) concentration was not measured or estimated due to the challenges and limitations associated with online OiW monitoring [32]. Hence, in this paper, the recently developed hydrocyclone model from [33,34] will be utilized to quantify the riser-induced slug's impact on the OiW concentrations after the downstream separation processes.

Two separation performances will be evaluated by the models during the simulations. The first separation performance metric is concentration reducing separation efficiency

$$\varepsilon_{CRE} = 1 - \frac{C_u}{C_i}, \quad (1)$$

which describes the percentage of OiW concentration reduction from the hydrocyclone inlet to hydrocyclone underflow, where C_i and C_u are the volumetric OiW concentration at the inlet and underflow, respectively and Q_o and Q_i is the hydrocyclone inlet and overflow flow rate, respectively [35,36]. The second separation performance metric is the oil removal efficiency

$$\varepsilon_{ORE} = \frac{C_o Q_o}{C_i Q_i}, \quad (2)$$

which describes the volumetric percentage of oil that leaves the overflow [37,38].

The rest of the paper is organized as follows: Section 2 briefly describes the testing facility, Section 3 describes the mathematical model of the separation units, Section 4 describes the emulated and modelled scenarios with associated operation conditions, Section 5 examines the simulation results and finally a conclusion is carried out in Section 6.

2. Testing Facility

The testing facility described in this section is an extension of the facility examined in [39–41]. Figure 1 from [31] shows P&ID drawings of two parts of the laboratory testing facility where all the examined experiments are executed. The facility consists of a pipeline-riser-separator-hydrocyclone system in a complete flow-loop. Each individual part of system can be tested respectively. Figure 1a shows the pipeline-riser with the anti-slug control configuration examined in this paper, and Figure 1b illustrates the gravity separator with water level control loop and the hydrocyclone with the pressure drop ratio (PDR) control loop.

All data acquisition and control are performed using a standard PC running Simulink Real-time (xPC) through a target PC which guarantees real-time simulations. The transmitters and actuators are connected to the target PC through National Instruments (NI) data acquisition and output PCI cards, which are installed in an electrical distribution box. All input and output signals of the facility are sampled at 100 Hz.

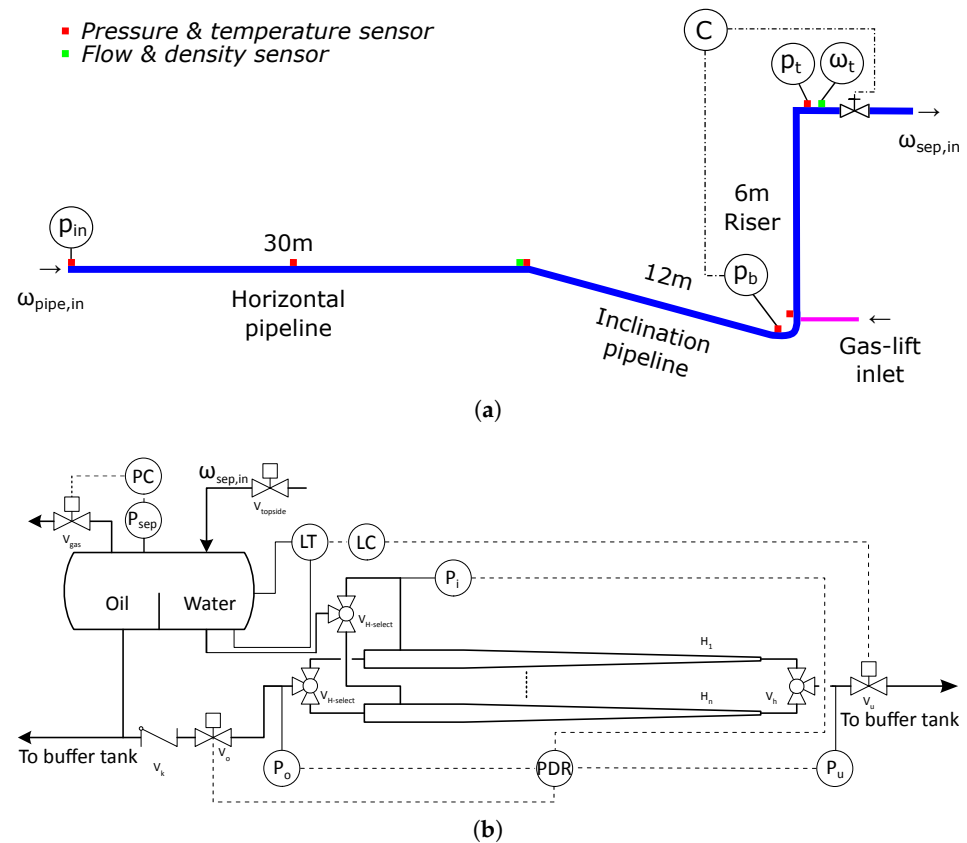


Figure 1. Two illustrations of the linked laboratory-scaled pipeline-riser and separator-hydrocyclone processes, including the respective control loops [31]. (a) The pipeline-riser section including the anti-slug controller actuates the topside choke valve with feedback data from P_b . The riser outlet ($\omega_{sep,in}$) is the inlet to the gravity separator. Furthermore, several unused pressure, temperature, flow and density measurements are available for monitoring the system. (b) The 3-phase gravity separator and deoiling hydrocyclone. The water level and PDR control loops are illustrated. Only one hydrocyclone (H_1) is applied in this paper. A more detailed separator and hydrocyclone laboratory description can be found in [29].

3. Model

This section describes the model framework for used in this paper. This model framework is based on previous works, which is well-described and validated in [33], expanded by a separator-tank model and two valve controllers. The model framework is illustrated in Figure 2.

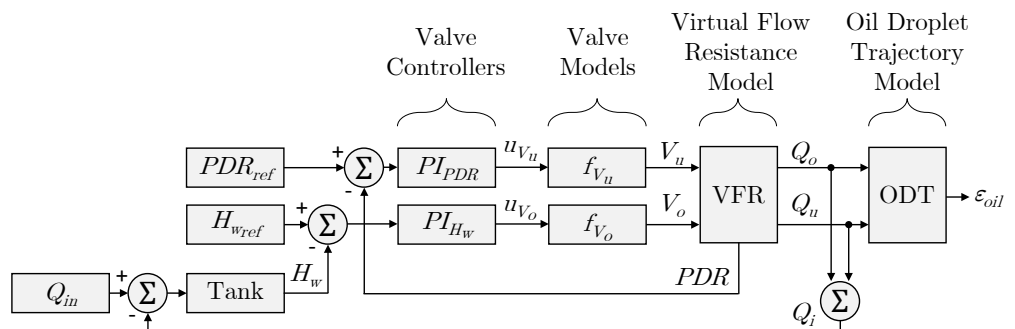


Figure 2. Overview of the model framework.

The flow rate of water entering the separator tank (Q_{in}) is a non-controllable input. The flow rate leaving the separator tank is the same flow rate that enters the hydrocyclone (Q_i). The opening degree of the underflow valve (V_u) is actuated by the water level

controller (PI_{H_w}), which aims to maintain a constant water level (H_w) at the water level reference ($H_{w_{ref}}$). The opening degree of the overflow valve (V_o) is actuated by the pressure difference ratio controller (PI_{PDR}), which aims to maintain a constant PDR at the PDR reference (PDR_{ref}). The two valve models f_{V_u} and f_{V_o} are modelled as first order transfer functions, to emphasize that the valves are physical systems that cannot move infinitely fast. A virtual flow resistance (VFR) model, proposed in [27], estimates the flow rates leaving the hydrocyclone: Underflow flow rate (Q_u) and overflow flow rate (Q_o). Finally, an oil droplet trajectory (ODT) model, proposed in [42], extended in [43], and validated in [33], estimates the deoiling performance of the hydrocyclone.

3.1. Separator Tank

The water level in the separator tank is modeled by the relationship between accumulated volume and water level of a horizontal cylinder tank:

$$\frac{dH_w}{dt} = (Q_{in} - Q_i) \frac{\sqrt{H_w(2r_T - H_w)}}{r_T^2 L_T (1 - \cos(2\cos^{-1}(\frac{r_T - H_w}{r_T})))} \tag{3}$$

where r_T and L_T are the radius and length of the horizontal cylinder, respectively. The accumulating volume is $Q_{in} - Q_i$ as Q_i is the flow rate entering the hydrocyclone.

3.2. Hydrocyclone Part 1: Virtual Flow Resistance

The hydrocyclone model for this work is divided into two parts, where the first part solves the relevant flow and pressures, and the second part computes oil droplet trajectories and estimates separation efficiency.

The relationship between the flow rates Q_i , Q_u , and Q_o and the pressures P_i , P_u , P_o , P_{ub} , and P_{ob} is approximated by three virtual orifice equations, two valve equations and the continuity equation $Q_i = Q_u + Q_o$, such that Q_u and Q_o and the internal pressures P_u and P_o can be solved at every time step. This system of pressure drops is illustrated in Figure 3.

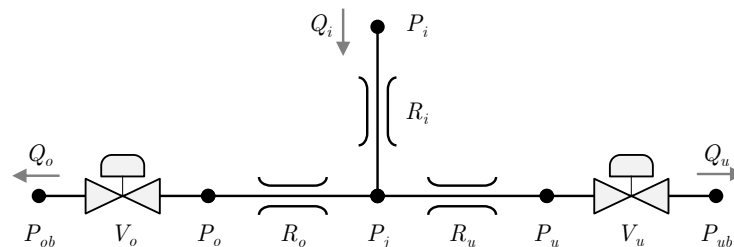


Figure 3. Hydrocyclone mathematically decomposed as simplified pressure drops. This figure is from [33].

The three virtual resistances $R_{i,u,o}$ are assumed governed by

$$\Delta P = \frac{Q^2}{K} \tag{4}$$

where ΔP is the pressure drop over a resistance, Q is the flow rate passing through it, and K its virtual flow permeability constant.

The pressure difference over the valves are assumed as

$$\Delta P_{V_u} = \frac{Q_u^2}{(K_{V_u} V_u)^2} \tag{5}$$

and

$$\Delta P_{V_o} = \left(\frac{Q_o}{K_{V_o1} V_o^{\frac{1}{2}}} \right)^2 + \frac{Q_o^2}{K_{V_o2}^2} \tag{6}$$

which are chosen to emulate the valve properties of the used pilot plant, as described in [33].

To solve this system of equations, the boundary pressures P_i, P_{ub}, P_{ob} are required to be known. The internal pressures are used to generate PDR by:

$$PDR = \frac{P_i - P_o}{P_i - P_u}, \tag{7}$$

which will be sent to PI_{PDR} to be used as feedback.

3.3. Hydrocyclone Part 2: Oil Droplet Trajectory

With Q_u and Q_o defined, the ODT model estimates the velocity fields inside the hydrocyclone geometry and computes the oil droplets' trajectory to evaluate the deoiling performance as extensively described in [33].

The principle of the model is to estimate ϵ_{ORE}

$$\epsilon_{ORE} = \int_0^\infty G(D)\phi_i(D)dD, \tag{8}$$

where D is droplet size and $G(D)$ is the grade efficiency, also known as mitigation probability. G is estimated based on droplet trajectories [33]. To compute these trajectories, Q_u and Q_o from the VFR model are needed to solve the estimations of the velocity fields inside the hydrocyclone.

4. Scenario Design

The scenarios in this study are based on defined operating conditions, such as fixed pressurization of the separator and common controllers for both hydrocyclone and separator. Detailed description of the separation controllers can be found in Section 4.1 and description of the separator inflow conditions can be found in Section 4.2.

4.1. Separation Dimensions and Controllers

Common for all scenarios are the controllers as listed in Table 1. The separator tank has the following dimensions: $L_T = 1.5$ m and $r_T = 0.3$ m and the separator pressure controller (controlled by the gas outlet valve) is fast compared to the dominant dynamics, such that the tank pressure is assumed constant. For all the scenarios, $P_i = 7$ bar.

Table 1. Common controller description.

Controller	PI_{PDR}	PI_{H_w}
Control variable	u_{V_o}	u_{V_u}
Process variable	PDR	H_w
Controller type	PI	PI
Controller coefficients	$P = 0.011; I = 0.067$	$P = 81.08; I = 1.466$
Setpoint	2.5	0.25 m

The droplet size distribution of the mixture entering the hydrocyclone (ϕ_i) is assumed as a time invariant random variable distributed according to a log-normal distribution with mean 20 μm and variance 0.0005 μm^2 . The inlet oil concentration is assumed to be 400 ppm and constant for both experiments.

4.2. Separator Inflow Generation

The scenarios included in this paper are based on the inlet operation conditions to the separator. Three different flow conditions are considered: 1. No control, where there are fluctuating slug flow, 2. Open-loop anti-slug control where the topside valve located upstream the separator is choked below the bifurcation point, and 3. closed-loop anti-slug control, where P_b is used as a feedback signal for actuating the valve.

The slugs are generated from the flow conditions from [31] (scenario 1), where a typical severe slug scenario is emulated in the same testing facility as used in this study; see Section 2. Only the flow and pressure conditions are required for simulating the impact on the downstream 3-phase separator and hydrocyclone. Therefore, the time series are included as inputs to the separator and hydrocyclone models instead of the actual slug model (described, identified and validated in [44]). Two tests are considered: One open- and one closed-loop anti-slug control test, respectively.

- An open-loop anti-slug experiment is shown in Figure 4, where $t < 400$ s is slug flow and $t > 400$ s is bubble flow caused by choking below the bifurcation point of the topside valve located upstream the separator.
- A closed-loop anti-slug control experiment is shown in Figure 5, where the controller activated at $t = 400$ s eliminates the slug flow until it is given a infeasible setpoint step at 975 s which caused the anti-slug controller to fail at stabilizing the flow and pressure. The setpoint given at $t > 975$ s cannot be attained due to the control valve saturation constraints of $0\% \leq V_{topside} \leq 100\%$.

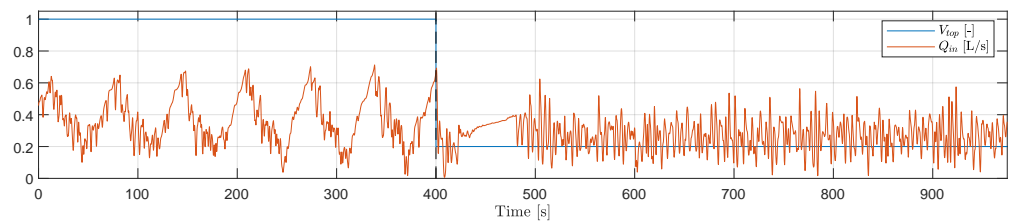


Figure 4. Shows Q_{in} and V_{top} during experiment 1. V_{top} starts fully open and reduces its opening degree to 20% open at 400 s. As a result, the slug is eliminated.

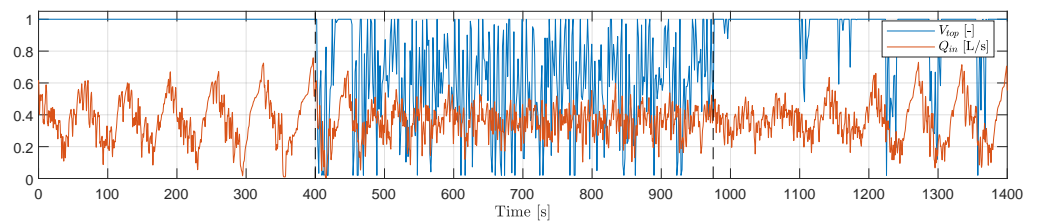


Figure 5. Shows Q_{in} of experiment 2. The anti-slug controller, which actuates V_{top} using P_{bt} as feedback, is enabled at 400 s. As a result, the amplitude of the slug cycles are reduced. As the slugging conditions becomes increasingly more severe, V_{top} saturates at 975 s which reduces the controller's slug suppression. As a result, the amplitude of the slug cycles increases at $t > 975$ s.

The two experiments (in the following referred to as experiment 1 and 2, respectively), have different lengths, and thus, in Section 5 experiment 1 ends at $t = 975$ s, which is exactly the point where the closed-loop controller changes setpoint and becomes unstable in experiment 2.

5. Simulation Results

This section presents the results from the two simulations using Q_{in} obtained from the inflow experiments examined in Section 4.2 with the operating conditions and controllers described in Section 4.1. All the results examined in this section are summarized in Table 2 where the steady-state results of experiment 1 and 2 are compared, where experiment 1 is separated into uncontrolled (100% valve opening) and open-loop control (20% valve opening) and experiment 2 is separated into closed-loop I, where the anti-slug controller works, and closed-loop II, where the change in the anti-slug controller's setpoint causes the slug reoccur.

Table 2. Scenario comparison.

	Unit	Uncontrolled	Open-Loop	Closed-Loop I	Closed-Loop II
Experiment	-	1	1	2	2
Slugging	-	Yes	No	No	Yes
t_{start}	s	246	600	600	1250
t_{end}	s	372	900	900	1380
Q_{in}	L/s	0.375	0.263	0.357	0.366
Q_i	L/s	0.376	0.262	0.359	0.367
Q_u	L/s	0.364	0.254	0.347	0.355
Q_o	L/s	0.012	0.009	0.012	0.012
V_u	%	38.7	32.5	38.3	38.2
V_o	%	1.2	0.4	0.8	1.14
PDR^*	-	2.5 ± 0.185	2.5 ± 0.03	2.5 ± 0.06	2.5 ± 0.185
F_s	%	3.22	3.24	3.25	3.22
C_u^*	ppm	71.2 ± 23.4	84.3 ± 4.80	67.2 ± 4.84	72.2 ± 21.9
ϵ_{CRE}	%	82.2	78.9	83.2	82.0
ϵ_{ORE}	%	82.8	79.6	83.8	82.5

* The numeric value following \pm is the standard deviation.

The controller actuating V_u was able to maintain H_w within 2 mm from the 25 cm liquid height reference as seen in Figure 6. The largest deviations from the reference occur during the first 400 s of both experiments, and after 2000 s in experiment 2.

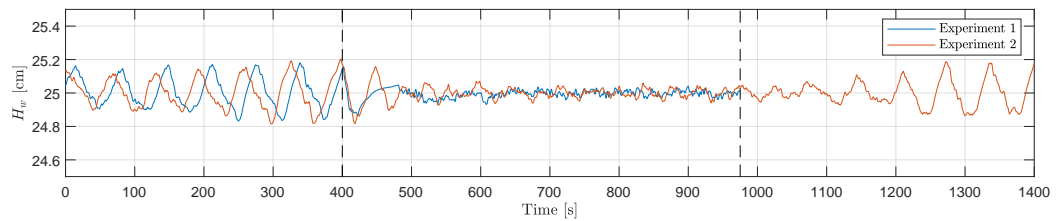


Figure 6. Shows H_w during both experiments.

Similarly, the controller actuating V_o was able to maintain its 2.5 PDR reference in the non-slugging period of both experiments, but had large relative deviations in the slugging periods of both experiments as seen in Figure 7. It is clear that the PDR oscillations are relatively larger than H_w , however, this is a consequence of the impact from varying inflow to the hydrocyclone from the separation. This is clear from Figure 8 where fast reference tracking of the level controller results in Q_i very similar to Q_{in} during both experiments. Hence, if the H_w PI controller coefficients are decreased the oscillations will increase for H_w and decrease for PDR. A tradeoff between the two responses must therefore be made, and in this study the tradeoff is based on knowledge from offshore oil and gas operators in the North Sea which both the experiments and simulations are intended to emulate.

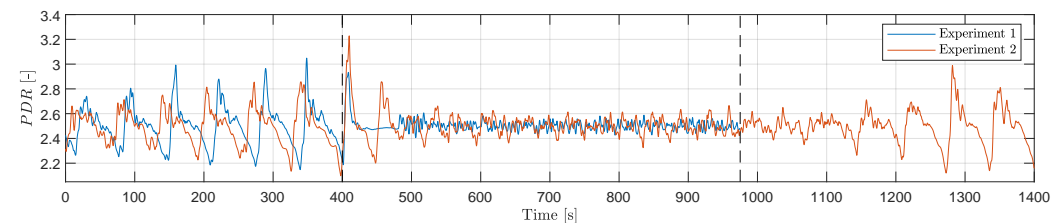


Figure 7. Shows PDR during both experiments. PDR has fluctuations that follow the slug cycles before V_{top} closes from 100% to 20%. After 400 s, the fluctuations of PDR are reduced. For experiment 2, the fluctuations of PDR are reduced as the controller actuating V_{top} is enabled at 400 s. After 1000 s where V_{top} is saturated most of the time, the fluctuations of PDR increase.

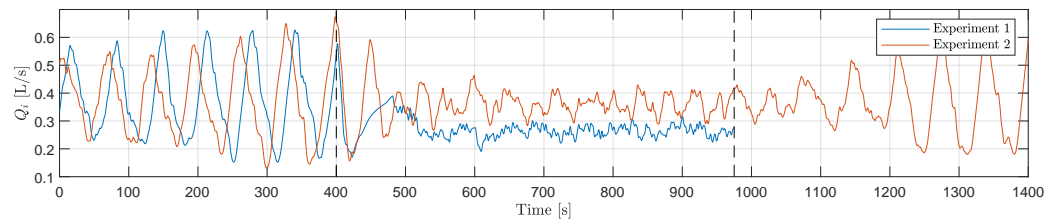


Figure 8. Flow entering the hydrocyclone during both experiments.

The opening degree of V_u and V_o during both experiments are shown in Figure 9. As low flow rate is required to recreate slugging conditions, V_o operates at low openings around 1%, whereas V_u operates around 30% to 50% open. This operational range of the valves are a consequence of the physical testing facility, where the flow rate range that result in slugging flow is governed by the 6 m riser [31,44]. Although this is clearly not in the optimal operational range of the hydrocyclone, it is still sufficient for quantifying the severe slug’s impact to the separation compared to non-slug, however, the absolute separation efficiency can be improved in both experiments by increasing inflow rates and separator pressurization.

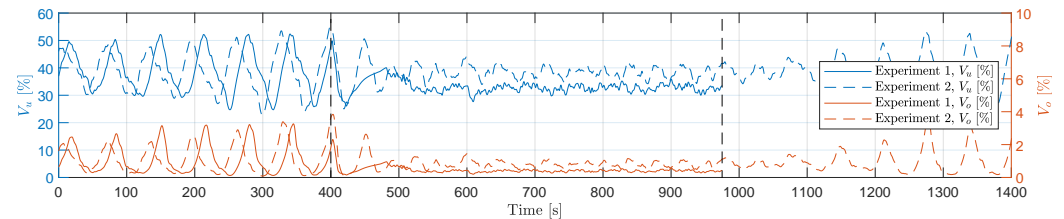


Figure 9. Hydrocyclone valve openings during both experiments.

During both experiments, the underflow OiW concentration from about 45 ppm to 125 ppm and with the largest fluctuations occurring during the slugging periods as seen in Figure 10. The closed-loop slug elimination is clearly superior to the open-loop elimination although both approaches stable inflow conditions to the separator and hydrocyclone. Hence, the lower inflow rate caused by open-loop choking clearly decrease the separation efficiency, due to the hydrocyclone’s demand for not only constant, but also larger, inflow rates from the separator. Moreover, it is clear that the OiW concentration follows the slug frequency, which again demonstrates that the hydrocyclone is inflow sensitive. This applies for both the uncontrolled part of experiment 1 and 2 and the closed-loop II part. From Table 2 it is observed that the average values of C_u are primarily linked to the flow rates, where the standard deviations are linked to the oscillations in flow and, thus, whether slug occurs or not.

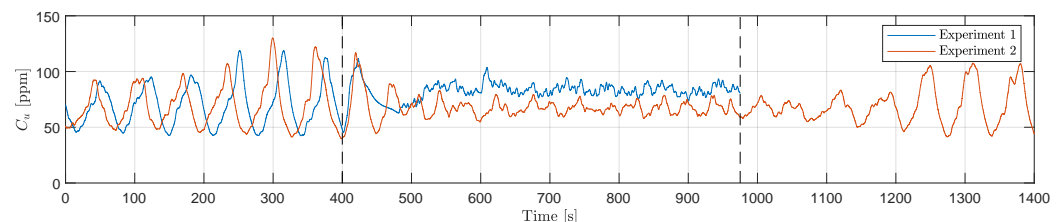


Figure 10. Underflow OiW concentration during both experiments.

Equivalently, the concentration reducing efficiency and the volumetric oil removal efficiency during both experiments are shown in Figures 11 and 12 respectively. As expected the two graphs follow Figure 10 while it is observed that both efficiencies fluctuate between approximately 70 and 90%. This is a low efficiency range compared to typical offshore processes, but it is important to highlight that the absolute concentration cannot be directly compared to real facilities due to the laboratory scaling and the bounded operating

conditions. Table 2 shows the average efficiencies and it is surprising that Closed-loop II has similar efficiencies to Uncontrolled as the Uncontrolled has significantly larger inflow rates to the separator which intuitively should result in better operating conditions for the hydrocyclone. However, it can be seen that Closed-loop I provides the best and Open-loop provides the worst separation performance.

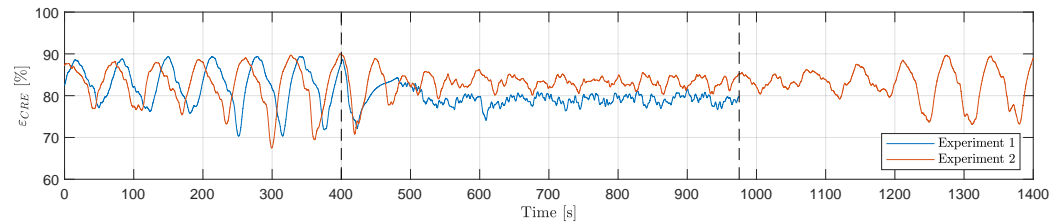


Figure 11. Concentration reduction efficiency during both experiments.

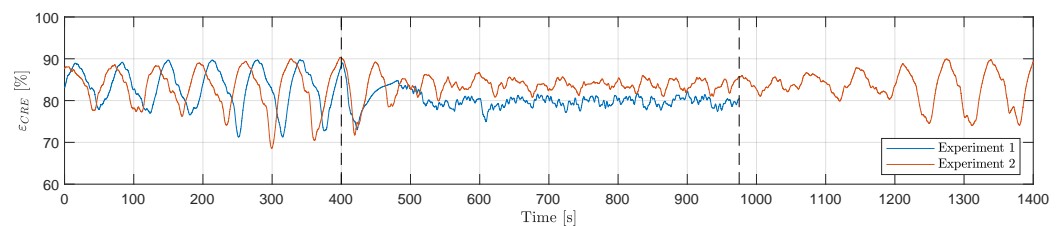


Figure 12. Oil removal efficiency during both experiments.

Figure 13 shows the average oil droplet distributions of the four scenarios as well as the droplet distribution entering the hydrocyclone from the separator. Open-loop causes the largest droplets on average, while Closed-loop I both provides the smallest droplet diameters on average as well as the smallest standard deviation.

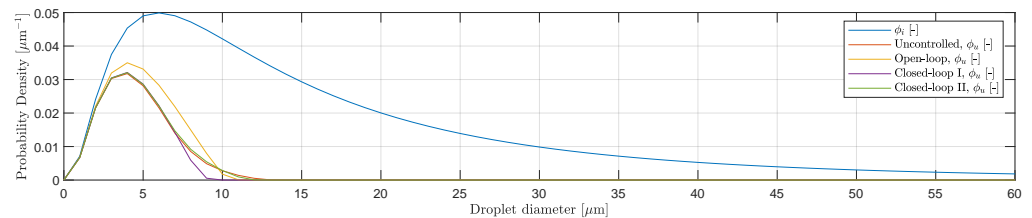


Figure 13. Average oil droplet distributions of the four scenarios.

Figure 14 visualises the OiW concentration distributions. Here, it is obvious that the slug present in both Uncontrolled and Closed-loop II leads to flat broader curve, while the non-slug in both Open-loop and Closed-loop I has a narrower span. In reality, operators are interested in keeping the OiW concentrations on the underflow as stable as possible due to issues related to OiW monitoring and the severe negative impact to the environment of large OiW concentrations discharged into the ocean, even for a short time period. Hence, even though the Open-loop scenario clearly increases the average OiW concentration it might be preferred over the alternatives where slug is present. Still, Closed-loop I is the best of all the four scenarios on both parameters.

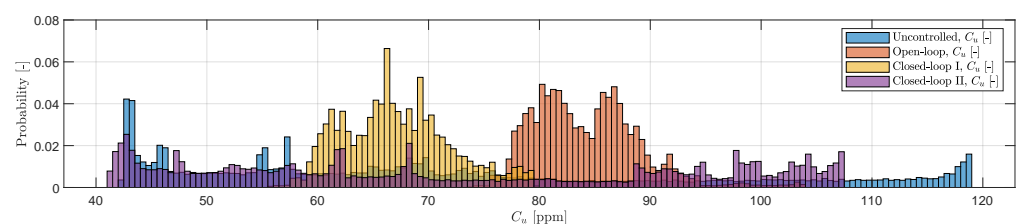


Figure 14. Underflow OiW concentration distributions of the four scenarios.

6. Conclusions and Future Work

Previous work on slugging suppression by actuating the topside valve using the bottom riser pressure as feedback successfully concluded that the amplitude of the slugging can be reduced experimentally. However, the limitation of real-time OiW monitors, left an open question as to how much this affects the separation performance of the deoiling produced water treatment system, especially droplet diameter size, OiW concentrations and separation efficiency. To quantify the performance improvement, a grey-box model of the combined separator tank plus hydrocyclone was utilized and simulated under the same conditions as the previous experimental works.

The results demonstrate that the slug flow regime causes large variations in the OiW concentrations in the hydrocyclone's underflow. This applies both for the uncontrolled slug and the infeasible closed-loop slug control scenarios. The average flow rate entering the separator has a substantial impact on the separation efficiency, which is clear when comparing the open-loop and successful closed-loop anti-slug control methods. Here, the closed-loop approach is superior to the open-loop approach due to the lower flow caused by the choked valve. This can be explained from the hydrocyclone demand of both pressure and inflow from the separator for optimal operation.

It can be concluded that the riser-induced slugs cause large fluctuations following the slug frequency in OiW concentrations downstream the entire separation process, ultimately decreasing the separation efficiency. Moreover, the absolute flow rate into the separator significantly impacts the separation efficiency, which demand the anti-slug technique to not limit the production rate. This was demonstrated by the simple feedback controller which was superior to the open-loop slug elimination method.

Even though this work is based on a validated experimental test from [31] and a validated model from [34], the accuracy of model's parts and the experimental measurements can always benefit from further validation. In future work the simulations will be tested experimentally with real-time OiW monitors to further validate the results. Moreover, an extended separator model can be included for extending the separation efficiency of the separator and not only the hydrocyclone. Lastly, more advanced anti-slug controllers can be implemented to compare the control solution's impact on the downstream separation performance.

The main contributions of the paper can be summarized as:

- Four scenarios were experimental tested on a pilot plant emulating different multi-phase flow regimes and rates into a typical deoiling separation process. This differs from most existing literature where the separation units only have been examined isolated and not in combination [18–25].
- The experiments were used in combination with simulations to demonstrate how severe riser-induced slugs effect the OiW downstream the separation units. Measuring low OiW concentrations has many challenges and limitations [31,32], and therefore, a validated separator and hydrocyclone model were used to simulate the OiW concentration and droplet distribution.
- Although previous studies qualitatively showed that both the separators' and hydrocyclones' individual performances are linked to flow rates and pressure ratios [15,17], this study quantitatively examined these effects as well as the coupling between the units.

Author Contributions: Conceptualization, methodology, investigation, simulations, analysis and writing by S.P. and M.V.B. All authors have read and agreed to the published version of the manuscript.

Funding: This research received no external funding.

Institutional Review Board Statement: Not applicable.

Informed Consent Statement: Not applicable.

Data Availability Statement: The data presented in this study are available on request from the authors.

Acknowledgments: Thanks go to AAU colleagues: S. Jespersen, D. S. Hansen, L. Hansen, P. Durdevic and Z. Yang for many valuable discussions and technical support.

Conflicts of Interest: The authors declare no conflict of interest.

References

1. Havre, K.; Stornes, K.O.; Stray, H. Taming Slug Flow in Pipelines. 2000. Available online: https://folk.ntnu.no/skoge/publications/2000/havre_slugpaper/abbreviate4_00.pdf (accessed on 5 April 2021).
2. Pedersen, S.; Durdevic, P.; Yang, Z. Challenges in slug modeling and control for offshore oil and gas productions: A review study. *Int. J. Multiph. Flow* **2017**, *88*, 270–284. [[CrossRef](#)]
3. Pedersen, S.; Durdevic, P.; Yang, Z. Review of Slug Detection, Modeling and Control Techniques for Offshore Oil & Gas Production Processes. In Proceedings of the 2nd IFAC Workshop on Automatic Control in Offshore Oil and Gas Production, Florianópolis, Brazil, 27–29 May 2015; Volume 48, pp. 89–96.
4. Hill, T.J.; Wood, D.G. Slug flow: Occurrence, consequences, and prediction. In Proceedings of the University of Tulsa Centennial Petroleum Engineering Symposium, Tulsa, OK, USA, 29–31 August 1994.
5. Sun, J.Y.; Jepson, W.P. Slug Flow Characteristics and Their Effect on Corrosion Rates in Horizontal Oil and Gas Pipelines. *SPE* **24787** **1992**, 215–228. Available online: <https://onepetro.org/SPEATCE/proceedings-abstract/92SPE/All-92SPE/SPE-24787-MS/54277> (accessed on 5 April 2021).
6. Zhou, X.; Jepson, W.P. Corrosion in Three-phase Oil/Water/Gas Slug Flow in Horizontal Pipes. *NACE Int.* **1994**, *26*. Available online: <https://www.osti.gov/biblio/70033> (accessed on 5 April 2021).
7. Kang, C.; Wilkens, R.; Jepson, W.P. The Effect of Slug Frequency on Corrosion in High Pressure, Inclined Pipelines. *NACE Int.* **1996**, *20*. Available online: <https://onepetro.org/NACECORR/proceedings-abstract/CORR96/All-CORR96/NACE-96020/113050> (accessed on 5 April 2021).
8. Isaac, O.A.; Cao, Y.; Lao, L.; Yeung, H. Production Potential of Severe Slugging Control Systems. In Proceedings of the 18th IFAC World Congress, Milan, Italy, 28 August–2 September 2011; pp. 10869–10874.
9. Yang, Z.; Juhl, M.; Löhndorf, B. On the Innovation of Level Control of an Offshore Three-Phase Separator. In Proceedings of the 2010 IEEE International Conference on Mechatronics and Automation, Xi’an, China, 4–7 August 2010; pp. 1348–1353.
10. Pedersen, S.; Durdevic, P.; Yang, Z. Learning control for riser-slug elimination and production-rate optimization for an offshore oil and gas production process. In Proceedings of the 19th World Congress of the International Federation of Automatic Control, Cape Town, South Africa, 24–29 August 2014; pp. 8522–8527.
11. Jahanshahi, E.; Skogestad, S.; Helgesen, A.H. Controllability analysis of severe slugging in well-pipeline-riser systems. In Proceedings of the IFAC Workshop on Automatic Control in Offshore Oil and Gas Production, NTNU, Trondheim, Norway, 31 May–1 June 2012; pp. 101–108.
12. Jahanshahi, E. Control Solutions for Multiphase Flow: Linear and Nonlinear Approaches to Anti-Slug Control. Ph.D. Thesis, Department of Chemical Engineering, Norwegian University of Science and Technology, Trondheim, Norway, 2013.
13. Jansen, F.E.; Shoham, O.; Taitel, Y. The Elimination of severe slugging-experiments and modeling. *Int. J. Multiph. Flow* **1996**, *22*, 1055–1072. [[CrossRef](#)]
14. Nowakowski, A.F.; Cullivan, J.; Williams, R.; Dyakowski, T. Application of CFD to modelling of the flow in hydrocyclones. Is this a realizable option or still a research challenge? *Miner. Eng.* **2004**, *17*, 661–669. [[CrossRef](#)]
15. Husveg, T.; Rambeau, O.; Drengstig, T.; Bilstad, T. Performance of a deoiling hydrocyclone during variable flow rates. *Miner. Eng.* **2007**, *20*, 368–379. [[CrossRef](#)]
16. Husveg, T. *Operational Control of Deoiling Hydrocyclones and Cyclones for Petroleum Flow Control: Trygve Husveg*; Avhandling/Universitetet i Stavanger, University of Stavanger: Stavanger, Norway, 2007.
17. Wilhelmsen, M. Control Structure and Tuning Method Design for Suppressing Disturbances in a Multi-Phase Separator. Master’s Thesis, Department of Engineering Cybernetics, Norwegian University of Science and Technology, Trondheim, Norway, 2013.
18. Bradley, D. *The Hydrocyclone*, 1st ed.; Pergamon Press: Oxford, UK, 1965; Volume 4, p. 330.
19. Rietema, K. The mechanism of the separation of finely dispersed solids in cyclones. In *Cyclones in Industry*; Rietema, K., Verver, C., Eds.; Elsevier: Amsterdam, The Netherlands, 1961; Chapter 4, pp. 46–63.
20. Svarovsky, L.; Marasinghe, B. Performance of hydrocyclones at high feed solids concentrations. In *Proceedings of the 1st International Conference on Hydrocyclones, Cambridge, UK*; Priestley, G., Stephens, H., Eds.; Bhra Fluid Engineering: Cambridge, UK, 1980; pp. 127–142.
21. Bloor, M.; Ingham, D. On the efficiency of the industrial cyclone. *Trans. Inst. Chem. Eng* **1973**, *51*, 173–176.
22. Davidson, M.R. Similarity solutions for flow in hydrocyclones. *Chem. Eng. Sci.* **1988**, *43*, 1499–1505. [[CrossRef](#)]
23. Holland-Batt, A. A bulk model for separation in hydrocyclones. *Inst. Min. Metall.* **1982**, *91*.
24. Hsieh, K.T.; Rajamani, R.K. Mathematical model of the hydrocyclone based on physics of fluid flow. *AIChE J.* **1991**, *37*, 735–746. [[CrossRef](#)]
25. Rajamani, K.; Hsieh, K. Hydrocyclone model: A fluid mechanic approach. In Proceedings of the SME Annual Meeting, Phoenix, AZ, USA, 25–28 January 1988; Smith, S.G.D., Ed.; Society of Mining Engineers of AIME: Luxembourg, 1988; p. 88.
26. Meldrum, N. Hydrocyclones: A Solution to Produced-Water Treatment. *SPE Prod. Eng.* **1988**, *3*, 669–676. [[CrossRef](#)]

27. Bram, M.V.; Hansen, L.; Hansen, D.S.; Yang, Z. Grey-Box modeling of an offshore deoiling hydrocyclone system. In Proceedings of the 2017 IEEE Conference on Control Technology and Applications (CCTA), Mauna Lani, HI, USA, 27–30 August 2017; pp. 94–98. [\[CrossRef\]](#)
28. Durdevic, P.; Pedersen, S.; Bram, M.; Hansen, D.; Hassan, A.; Yang, Z. Control Oriented Modeling of a De-oiling Hydrocyclone. *I F A C Workshop Ser.* **2015**, *48*, 291–296. [\[CrossRef\]](#)
29. Durdevic, P.; Pedersen, S.; Yang, Z. Evaluation of OiW Measurement Technologies for Deoiling Hydrocyclone Efficiency Estimation and Control. In Proceedings of the OCEANS'16 MTS/IEEE, Shanghai, China, 10–13 April 2016.
30. Pedersen, S.; Durdevic, P.; Stampe, K.; Pedersen, S.; Yang, Z. Experimental Study of Stable Surfaces for Anti-Slug Control in Multi-phase Flow. *Int. J. Autom. Comput.* **2016**, *13*, 81. [\[CrossRef\]](#)
31. Pedersen, S.; Durdevic Løhndorf, P.; Yang, Z. Influence of riser-induced slugs on the downstream separation processes. *J. Pet. Sci. Eng.* **2017**, *154*, 337–343. [\[CrossRef\]](#)
32. Hansen, D.; Bram, M.; Lauridsen, S.; Yang, Z. Online Quality Measurements of Total Suspended Solids for Offshore Reinjection: A Review Study. *J. Clean. Prod.* **2020**, *14*, 967.
33. Bram, M.V.; Jespersen, S.; Hansen, D.S.; Yang, Z. Control-Oriented Modeling and Experimental Validation of a Deoiling Hydrocyclone System. *Processes* **2020**, *8*, 1010. [\[CrossRef\]](#)
34. Bram, M.V. Greybox Modeling and Validation of Deoiling hydrocyclones. Ph.D. Thesis, Aalborg University, Aalborg, Denmark, 2020.
35. Plitt, L.R. A Mathematical Model of The Hydrocyclone Classifier. *Miner. Process.* **1976**, *69*, 114–123. [\[CrossRef\]](#)
36. Colman, D.; Thew, M. Correlation of separation results from light dispersion hydrocyclones. *Chem. Eng. Res. Des.* **1983**, *61*, 233–240.
37. Svarovsky, L.; Svarovsky, J. A New Method of Testing Hydrocyclone Grade Efficiencies. In *Hydrocyclones*; Springer: Berlin/Heidelberg, Germany, 1992; pp. 135–145. [\[CrossRef\]](#)
38. Kharoua, N.; Khezzar, L.; Nemouchi, Z. Hydrocyclones for De-oiling Applications—A Review. *Pet. Sci. Technol.* **2010**, *28*, 738–755. [\[CrossRef\]](#)
39. Pedersen, S. Plant-Wide Anti-Slug Control for Offshore Oil and Gas Processes. Ph.D. Thesis, Aalborg University, Aalborg, Denmark, 2016. [\[CrossRef\]](#)
40. Biltoft, J.; Hansen, L.; Pedersen, S.; Yang, Z. Recreating Riser Slugging Flow Based on an Economic Lab-sized Setup. *IFAC Int. Workshop Period. Control.* **2013**, *5*, 47–52. [\[CrossRef\]](#)
41. Durdevic, P. Real-Time Monitoring and Robust Control of Offshore De-oiling Processes. Ph.D. Thesis, Aalborg University, Aalborg, Denmark, 2017.
42. Bram, M.V.; Hansen, L.; Hansen, D.S.; Yang, Z. Hydrocyclone Separation Efficiency Modeled by Flow Resistances and Droplet Trajectories. *IFAC-PapersOnLine* **2018**, *51*, 132–137. [\[CrossRef\]](#)
43. Bram, M.V.; Hansen, L.; Hansen, D.S.; Yang, Z. Extended Grey-Box Modeling of Real-Time Hydrocyclone Separation Efficiency. In Proceedings of the 2019 18th European Control Conference (ECC), Naples, Italy, 25–28 June 2019; pp. 3625–3631. [\[CrossRef\]](#)
44. Pedersen, S.; Jahanshahi, E.; Yang, Z.; Skogestad, S. Comparison of Model-Based Control Solutions for Severe Riser-Induced Slugs. *Energies* **2017**, *10*, 1014. [\[CrossRef\]](#)